shortening has been reported (Benetti et al., 2007). A mouse mutant deficient in telomere-elongating activity, *terc*$^{-}$/*terc*$^{-}$, yields detectable telomere shortening in descendent generations with increased subtelomeric hypomethylation (Benetti et al., 2007). In humans, mutations in DNA methyltransferase (DNMT3B) lead to the autosomal-recessive ICF (immunodeficiency, centromeric region instability, facial anomalies) syndrome (Hansen et al., 1999). The subtelomeric regions in lymphoblastoid and fibroblast cells of ICF patients are hypomethylated (Yehezkel et al., 2008). The telomeres in this syndrome are also abnormally short (Yehezkel et al., 2008). These observations thus lead to our hypothesis that aging-associated telomere shortening is related to an alteration of the subtelomeric methylation status in humans, and that disease conditions such as PD may accelerate this process.

MATERIALS AND METHODS

Study Population

Female patients with PD in Beppu city area who visited the outpatient clinic of the Kyushu University Beppu Hospital from November 2008 through December 2010 were enrolled in our telomere study, and female family members and female hospital staff members were also enrolled as the healthy controls. Seventeen patients with PD were enrolled. The participants ranged in age from 47 to 61 years. In addition, 20 healthy control participants (49–62 years old) were enrolled. To minimize the confounding effects influencing telomere length, we set the following criteria for the enrollment of the participants of this study. The inclusion criteria for patients with PD were (1) Japanese female; (2) de novo patients with PD diagnosed according to the UK Parkinson's Disease Society Brain Bank criteria; (3) stage 1 or stage 2 of the Hoehn-Yahr classification system; (4) nonsmokers; and (5) no abnormality in a regular medical check-up (including the checks of body mass index, blood pressure, fasting blood sugar, serum lipids, serum protein, C-reactive protein, and blood cell counts) within a year before the enrollment. The exclusion criteria for patients with PD were (1) non-Japanese; (2) male; (3) non-PD patients; (4) previously treated with anti-Parkinson drugs; (5) stage 3 or stage 4 of the Hoehn-Yahr classification system; (6) smokers; and (7) abnormality pointed out in a regular medical check-up within a year before the enrollment. The inclusion criteria for healthy control participants were (1) Japanese female; (2) nonsmokers; and (3) no abnormality in a regular medical check-up within a year before the enrollment and under no regular medication. The exclusion criteria for healthy control participants were (1) non-Japanese; (2) male; (3) smokers; and (4) abnormality pointed out in a regular medical check-up within a year before the enrollment or under a regular medication. We reconfirmed that the patients with PD and the healthy participants were in a similar medical condition by measuring clinical laboratory data (see Table 1). This research study was approved by the Conjoint Health Research Ethics Board of Kyushu University, and written consent was obtained from all of the participants. We also collected data to assess how many participants, who had never took hypnotic medicine for at least a year before the enrollment, took hypnotic medicine for insomnia at least once within 6 months after the enrollment as a measure of the presence of mental stress. This is a prospective case-controlled pilot study, and therefore no power analysis was performed. Blood samples were collected from the patients prior to administration of anti-Parkinson agents. Blood samples were drawn using heparinized syringes and 10-mL Vacutainer tubes. We diluted the sample with 20 times the volume of 10 mM Tris-HCl, 1 mM EDTA (pH 8.0) to remove erythrocytes through osmotic lysis. Next, peripheral leukocytes were collected by centrifugation.

Telomere Detection

Telomere detection was performed as previously described with modifications (Maeda et al., 2009). The methylation-sensitive and -insensitive isoschizomers *Hpa*II and *Msp*I were used. Both enzymes recognize and cut the tetranucleotide CCGG, but *Hpa*II does not cut CCGG when the center dinucleotide CG is methylated. Briefly, DNA was

Table 1. The comparison of the clinical data between patients and controls.

	Patients ($n = 17$)	Controls ($n = 20$)	p value
Age (years)	57.4 ± 4.4	55.8 ± 4.2	0.268
SBP (mm Hg)	122 ± 14	123 ± 17	0.926
DBP (mm Hg)	73 ± 11	71 ± 14	0.815
BMI	22.2 ± 3.0	22.3 ± 3.5	0.900
T-chol (mg/dL)	192 ± 31	185 ± 31	0.467
HDL (mg/dL)	66 ± 18	60 ± 14	0.330
LDL (mg/dL)	105 ± 25	100 ± 27	0.640
TG (mg/dL)	99 ± 27	104 ± 34	0.600
TP (g/dL)	7.1 ± 0.7	6.9 ± 0.5	0.200
Albumin (g/dL)	4.0 ± 0.4	3.9 ± 0.4	0.311
FBS (mg/dL)	92 ± 14	93 ± 11	0.805
CRP (mg/dL)	0.09 ± 0.07	0.07 ± 0.06	0.494
WBC (/mm^3)	4980 ± 2570	5260 ± 1090	0.663
RBC ($\times 10^4$/mm^3)	422 ± 38	407 ± 34	0.194
Hb (g/dL)	13.0 ± 1.1	12.5 ± 0.8	0.152
Hypnotic pill (%)	63%	26%	0.016

Note. SBP = systolic blood pressure; DBP = diastolic blood pressure; BMI = body mass index; T-chol = total cholesterol; HDL = high-density lipoprotein cholesterol; LDL = low-density lipoprotein cholesterol: TG = triglyceride; TP = total protein; FBS = fasting blood sugar; CRP = C-reactive protein; WBC = white blood cell count; RBC = red blood cell count; Hb = hemoglobin. Hypnotic pill = the percentage of subjects took a hypnotic pill more than once for 6 months after the enrollment.

extracted from peripheral blood leukocytes and the DNA (0.1 μg) was digested at 37°C with 1 U *Msp*I or *Hpa*II for 2 h. The digests (10 μL) were resolved by agarose gel-electrophoresis. The blotted DNAs were hybridized to a hypersensitive probe of 500-bp (TTAGGG)n labeled with digoxigenin, and then incubated with anti-digoxigenin-AP (alkaline phosphatase) specific antibody. The telomere probe was visualized by CSPD (disodium 3-(4-methoxy-spiro {1,2-dio-xetane-3,2'-(5'-chloro) tricyclo[3.3.1.1] decan}-4-yl) phenyl phosphate) provided with DIG Luminescent Detection Kit (Roche Diagnostics Japan, Tokyo, Japan). The smears of the autoradiogram were captured on an Image Master, and the telomere length was then assessed quantitatively. Every sample was measured in duplicate from the DNA digestion step.

Terminal Restriction Fragment (TRF) Analysis

The telomere length distribution was analyzed by comparing the telomere length using a telomere percentage analysis with three intervals of length as defined by a molecular weight standard as previously described (Maeda et al., 2009). The intensity was quantified as follows: each telomeric sample was divided into grid squares as follows according to the molecular size ranges derived from λ phage DNA-HindIII digest: >9.4, 9.4–4.4, and <4.4 kb. The percent of each molecular weight range was measured ([intensity of a defined region − background] × 100/[total lane intensity − background]). The mean terminal restriction fragment (TRF) lengths were estimated using the formula $\sum(OD_i - \text{background})/\sum(OD_i - \text{background}/L_i)$ (Maeda et al., 2009), where OD_i is the chemiluminescent signal and L_i is the length of the TRF fragment at position *i*. Subtelomeric methylation was assessed by comparing *Msp*I-TRF and *Hpa*II-TRF and by comparing *Msp*I telomere length distribution and *Hpa*II telomere length distribution. The difference between the percent of *Msp*I (*%Msp*I-TRF) and the *Hpa*II (*%Hpa*II-TRF) in each molecular weight range was calculated. The proportion of the calculated difference (*%Hpa*II-TRF − *%Msp*I-TRF) in the >9.4 kb range to *%Hpa*II-TRF in the >9.4 kb range ((*Hpa*II − *Msp*I)/*Msp*I(>9.4 kb)) was used to evaluate the methylation status of telomeres longer than 9.4 kb. Similarly, the proportion of the calculated difference (*%Msp*I-TRF − *%Hpa*II-TRF) in <4.4 kb range to *%Msp*I-TRF in <4.4 kb range ((*Msp*I − *Hpa*II)/*Hpa*II(<4.4 kb)) was used to evaluate the methylation status of telomeres shorter than 4.4 kb.

Statistical Analysis

The difference in the mean TRF length and a telomere percentage analysis with age were analyzed using a two-way analysis of variance (ANOVA). The data are shown using the mean ± standard deviation bars. The criterion for significance is $p < 0.05$. All analyses were carried out using the Sigma Statistical Analysis software program (Sigma 2.03, 2001; Sigma, St. Louis, MO).

RESULTS

We tried to detect PD-associated mental stress by assessing how many participants took sleeping pill(s) for insomnia at least once for 6 months after the enrollment in controls and patients with PD. Hypnotic pills were prescribed for more patients with PD than controls (Table 1). The mean *Msp*I-TRF tended to be shorter in PD with a borderline significance, compared to controls. The difference between the mean *Msp*I-TRF and *Msp*I subtracted from *Hpa*II-TRF also tended to be smaller in PD, but there was no significance. The mean *Hpa*II-TRF was significantly shorter in PD (Figure 1).

The distributions were subdivided into three areas according to size ranges, >9.4, 9.4–4.4, <4.4 kb. An analysis of the *Msp*I-TRF length distribution showed that long telomeres (>9.4 kb) were decreased in PD compared to controls (Figure 2a). The shorter telomeres (9.4–4.4 and <4.4 kb) tended to increase in PD but there was no significance (Figure 2a). These results indicated that telomere length became shorter, and the longer telomeres were affected preferentially in PD. These PD-associated differences in the telomere length distribution were also observed in the *Hpa*II-TRF length distribution (Figure 2b). *Hpa*II − *Msp*I area (*%Msp*I-area subtracted from *%Hpa*II-area) of each size area was compared between controls and patients with PD (Figure 2c, d). The subtracted distribution, *Hpa*II-TRF distribution minus *Msp*I-TRF distribution, however, revealed no alteration of the methylated status in the total telomeres. However, the *Hpa*II − *Msp*I value is affected by two differential factors, differences in the telomere length

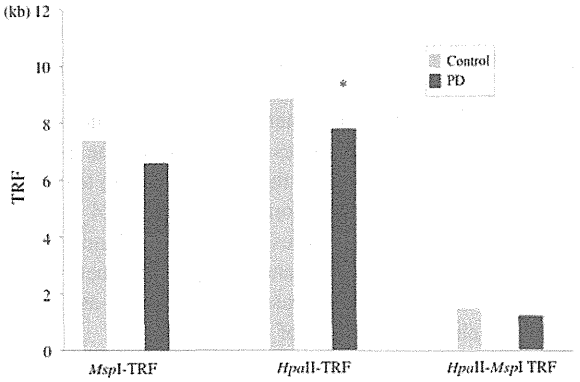

Figure 1. The mean telomere lengths (TRF) of *Msp*I and *Hpa*II TRF of controls and patients with PD are shown. The subtracted TRF is also shown. Vertical bars depict the standard deviations. *$p < 0.05$ vs. control.

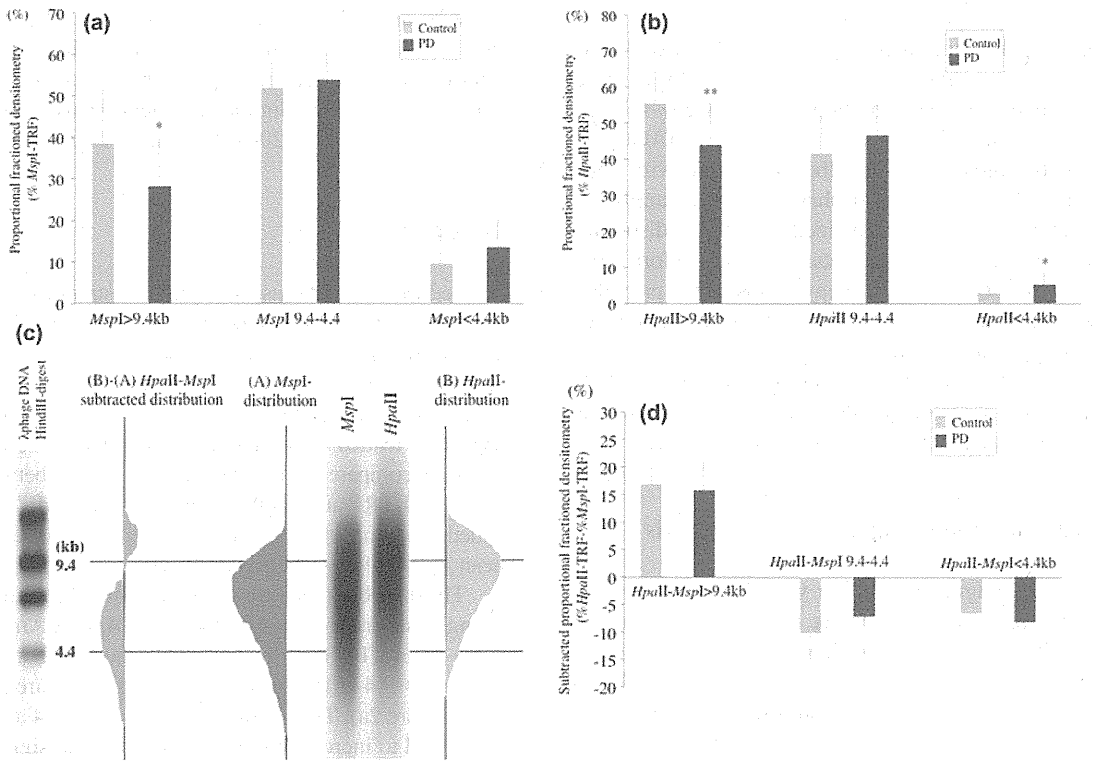

Figure 2. The *Msp*I- and *Hpa*II-TRF length distribution. Telomere fragment length percentage profiles are shown. The densitometry was examined for both cases of (**a**) *Msp*I and (**b**) *Hpa*II digestion. The densitometry data were then divided into three parts, >9.4, 9.4–4.4, and <4.4 kb. (**c**) A representative genomic Southern blot of leukocyte DNA with telomere probe using *Msp*I and *Hpa*II and the analysis of the *Hpa*II − *Msp*I subtracted TRF distribution. Densitometric curves are shown beside the Southern blot smear results. A subtracted distribution pattern calculated from subtraction of the two densitometries is shown on the left. (**d**) Subtracted value of the *Msp*I-TRF from the *Hpa*II-TRF densitometry in the three subdivided parts are shown as columns. The percentage of the respective area was presented as the fraction of the whole densitometric area (set as 100%). $*p < 0.05$; $**p < 0.01$.

and in the methylation status. In order to analyze the methylation status specifically, the methylation status was analyzed in long telomeres and short telomeres separately. The methylation-specific parameters, including the ratio of subtraction of *Msp*I-TRF lengths from *Hpa*II-TRF lengths of >9.4 kb and <4.4 kb to *Hpa*II-TRF lengths >9.4 kb and to *Msp*I-TRF lengths <4.4 kb, were calculated, respectively (Figure 3). The ratio of subtracted (*Hpa*II − *Msp*I)/HpaII(>9.4 kb) was significantly less in the patients with PD. This result suggested that short telomeres with hypomethylated subtelomeres decreased in the patients with PD. In summary, in PD the amount of long telomeres (>9.4 kb) decreased and short telomeres (<4.4 kb) with hypermethylated subtelomeres decreased. The analysis of telomere length distribution and subtelomeric methylation status is a more sensitive measure to detect PD-associated telomeric changes than that of mean TRF.

DISCUSSION

In the telomere length population of somatic cells, telomeres become shorter, and the shorter telomeres accumulate and increase as systemic aging proceeds. It has been reported that somatic telomere length is affected by metabolic conditions, such as blood sugar, serum cholesterol, and blood pressure (Uziel et al., 2007; Dei Cas et al., 2011;

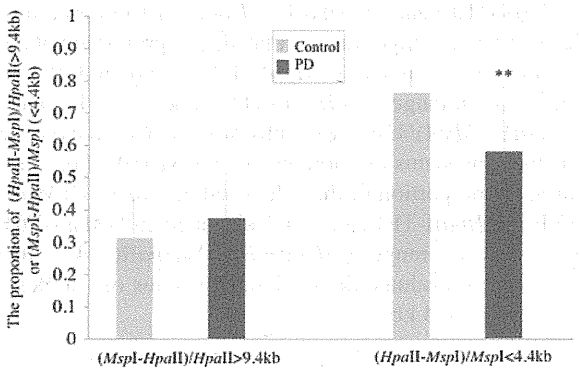

Figure 3. The relative methylation status of subtelomeres in PD. (*Hpa*II − *Msp*I)/HpaII (>9.4 kb) and (*Msp*I − *Hpa*II)/MspI (<4.4 kb) are used as indices indicating the subtelomeric methylation of longer (than 9.4 kb) and shorter (than 4.4 kb) telomeres, respectively. Vertical bars depict the standard deviations. $**p < 0.01$ vs. control.

Insel et al., 2011). In the present study, the metabolic data were similar between patients and controls. Therefore in the present analysis, the pathophysiological metabolic factors were removed to detect the difference of somatic telomere length between PD and controls. In order to detect the change of telomeric structure in PD, the mean telomere length, the telomere length distribution, and the subtelomeric methylation status were compared between healthy Japanese people and Japanese patients with PD. The present study showed that long telomeres decreased and subtelomeric methylaton of short telomeres decreased in female patients with PD. These observations suggest that the PD condition is associated with the attrition of long telomeres and the demethylation of the subtelomeres of short telomeres. These telomeric and subtelomeric alterations have been reported as a part of aging-associated alterations (Maeda et al., 2009). With aging, long telomeres increase, short telomeres increase, and the proportional subtelomeric methylation increases in long telomeres, and decreases in short telomeres. Accordingly, the PD condition seems to facilitate partly aging-associated telomere structural change. In mouse experiments, shortened telomeres and less methylation of the subtelomeric region of considerably shortened telomeres in the offspring of mice deficient in telomerase activity have been reported (Benetti et al., 2007). In human DNA methylase–deficient ICF syndrome, hypomethylated subtelomeres have been reported to be associated with enhanced telomeric shortening (Hansen et al., 1999; Yehezkel et al., 2008). These reports therefore suggest that subtelomeric hypomethylation is associated with telomeric attrition in somatic cells. The significant PD-associated alteration of subtelomeric methylation was observed limitedly in short telomeres (<4.4 kb), with no significant proportional increase of short telomeres. On the other hand, telomere attrition was prominent in long telomeres (>9.4 kb), with no significant change of subtelomeric methylation of long telomeres. Different from the aging-associated changes, the subtelomeric hypermethylation of long telomeres and the increase of short telomeres were not detectable. In PD, subtelomeric demethylation may be facilitated regardless of telomere length, and the amount of short telomeres did not increase possibly because of loss of short telomeres. One possible explanation for this observation is that cells bearing shorter telomeres with unmethylated subtelomeres in PD likely proceed faster into cell senescence. Neurodegenerative cell loss in PD is closely associated with oxidative stress as an etiopathological factor (Beal, 1995; Joseph et al., 1998). Oxidative DNA damage has been reported not only in neurons but also in the peripheral blood cells of patients with PD (Gao et al., 2003; Migliore et al., 2002; Vitte et al., 2004). The systemic oxidative stress is associated with PD pathogenesis and PD progression and is also reflected in telomere erosion. The mental stress in daily life is enhanced by PD symptoms including motor deficits and depression. Mental stress has been reported to enhance oxidative stress (Epel et al., 2004). Therefore, the observed telomere and subtelomere changes may occur from both oxidative damage (direct cause) and mental stress (secondary/indirect cause) of Parkinson's disease. Such stresses may cause fragility in the telomeric and subtelomereic structure in circulating leukocytes. Oxidative stress generates hydroxyl radicals, which can cause a wide range of DNA lesions such as nucleotide oxidation (Franco et al., 2008). Such DNA lesions have been shown to interfere with the access of the DNA methyltransferases, resulting in global hypomethylation (Kuchino et al., 1987; Hepburn et al., 1991; Xiao & Samson, 1993; Weitzman et al., 1994; Turk et al., 1995; Turk & Weitzman, 1995; Wachsman, 1997). The telomeric and subtelomeric regions impaired by oxidative stress progress to become hypomethylated and are open to easy access by oxygen radicals. Therefore, frequently evoked DNA damage in telomeres and subtelomeres by oxidative stress is thought to result in progressive hypomethylation in subtelomeres. This may explain why subtelomeres are hypomethylated, and cells containing short telomeres with hypomethylated subtelomeres are fragile in PD. From this viewpoint, the hypomethylated state of subtelomeres can be one of the potential markers for telomeric structural changes associated with PD. The differential contents of size-fractioned telomeres and the subtelomeric methylation status of short (<4.4 kb) telomeres are sensitive markers for PD-related genomic changes. Thus, somatic cells bearing short telomeres in PD are prone to enter the cell senescence state. Therefore the neuronal death of jeopardized neurons in the substantia nigra will be facilitated, and this will lead to PD progression. This progression may contribute to worsening of neurological symptoms (e.g., motor deficits), which may then increase mental stress in daily life. This secondary stress will cause further telomere attrition of somatic cells. This vicious cycle may contribute to accelerated PD progression in a subset of patients. Therapeutic approaches to lessen stress may therefore be beneficial to delay disease progression not only in PD but also in other chronic diseases where telomere shortening and the degeneration of somatic cells is present. Furthermore, telomeric changes may prove to be a useful biomarker to evaluate the effectiveness of therapeutic approaches in PD.

In conclusion, we demonstrated the presence of telomeric changes in peripheral leukocytes in PD. These new methods of analyzing telomere length distribution and subtelomric methylation may be effective tools to detect acceleration of aging-associated telomeric changes in other chronic diseases including other neurodegenerative disorders. Further study is necessary to confirm that these telomeric and subtelomeric alterations are commonly observed in neurodegenerative disorders. Some previous reports have described that patients with Alzheimer's disease bear shorter telomere lengths (Panossian et al., 2003). This telomere shortening in Alzheimer's disease may be accompanied by alterations in telomere length

distribution and subtelomeric methylation status. In addition, analyses of telomeric and subtelomeric changes of in vitro cultured cells entering the senescence state induced by hyperoxidative conditions would be helpful to clarify whether hyperoxidative conditions induce alterations in telomere length distribution and subtelomeric methylation.

ACKNOWLEDGMENTS

This work was supported by grants from the Ministry of Education, Science, and Culture of Japan (no. 23590885) and the National Natural Science Fund (NSFC) (no. 81170329/H2501). The authors thank Ms. Ueda and Ms. Taguchi for their valuable technical assistance. The authors are also grateful to Mr. Brian Quinn for his linguistic advice on the manuscript.

Declaration of interest: The authors report no conflicts of interest. The authors alone are responsible for the content and writing of the paper.

REFERENCES

Allsopp, R. C., Vaziri, H., Patterson, C., Goldstein, S., Younglai, E. V., Futcher, A. B., Greider, C. W., & Harley, C. B. (1992). Telomere length predicts replicative capacity of human fibroblasts. *Proc Natl Acad Sci U S A, 89*, 10114–10118.

Beal, M. F. (1995). Aging, energy, and oxidative stress in neurodegenerative diseases. *Ann Neurol, 38*, 357–366.

Beal, M. F. (2003). Mitochondria, oxidative damage, and inflammation in Parkinson's disease. *Ann N Y Acad Sci, 991*, 120–131.

Blackburn, E. H. (1991). Structure and function of telomeres. *Nature, 350*, 569–573.

Benetti, R., García-Cao, M., & Blasco, M. A. (2007). Telomere length regulates the epigenetic status of mammalian telomeres and subtelomeres. *Nat Genet, 39*, 243–250.

Dei Cas, A., Spigoni, V., Franzini, L., Preti, M., Ardigò, D., Derlindati, E., Metra, M., Monti, L. D, Dell'era, P., Gnudi, L., & Zavaroni, I. (2011). Lower endothelial progenitor cell number, family history of cardiovascular disease and reduced HDL-cholesterol levels are associated with shorter leukocyte telomere length in healthy young adults. *Nutr Metab Cardiovasc Dis,* 2011 Aug 6. [Epub ahead of print]

Epel ES, Blackburn EH, Lin J, Dhabhar FS, Adler NE, Morrow JD, et al. (2004). Accelerated telomere shortening in response to life stress. *Proc Natl Acad Sci U S A, 101*, 17312–17315.

Franco, R., Schoneveld, O., Georgakilas A. G., & Panayiotidis, M. I. (2008). Oxidative stress, DNA methylation and carcinogenesis. *Cancer Lett, 266*, 6–11.

Gao, H. M., Liu, B., Zhang, W., & Hong, J. S. (2003). Novel anti-inflammatory therapy for Parkinson's disease. *Trends Pharmacol Sci, 24*, 395–401.

Hansen RS, Wijmenga C, Luo P, Stanek AM, Canfield TK, et al. (1999). The DNMT3B DNA methyltransferase gene is mutated in the ICF immunodeficiency syndrome. *Proc Natl Acad Sci U S A., 96*, 14412–14417.

Harley, C. B., Futcher, A. B., & Greider, C. W. (1990). Telomeres shorten during ageing of human fibroblasts. *Nature, 345*, 458-460.

Hepburn, P. A., Margison, G. P., & Tisdale M. J. (1991). Enzymatic methylation of cytosine in DNA is prevented by adjacent O6-methylguanine residues. *J Biol Chem, 266*, 7985–7987.

Hirsch, E. C., Breidert, T., Rousselet, E., Hunot, S., Hartmann, A., & Michel, PP. (2003). The role of glial reaction and inflammation in Parkinson's disease. *Ann N Y Acad Sci, 991*, 214–228.

Insel, K. C., Merkle, C. J., Hsiao, C. P., Vidrine, A. N., & Montgomery, D. W. (2011). Biomarkers for cognitive aging—Part I: Telomere length, blood pressure and cognition among individuals with hypertension. *Biol Res Nurs,* 2011 May 17. [Epub ahead of print]

Iwama H, Ohyashiki K, Ohyashiki JH, Hayashi S, Yahata N, Ando K, et al. (1998). Telomeric length and telomerase activity vary with age in peripheral blood cells obtained from normal individuals. *Hum Genet, 102*, 397–402.

Joseph, J. A., Denisova, N., Fisher, D., Bickford, P., Prior, R., & Cao, G. (1998). Age-related neurodegeneration and oxidative stress: Putative nutritional intervention. *Neurol Clin, 16*, 747–755.

Kuchino Y, Mori F, Kasai H, Inoue H, Iwai S, Miura K, et al. (1987). Misreading of DNA templates containing 8-hydroxydeoxyguanosine at the modified base and at adjacent residues. *Nature, 327*, 77–79.

Maeda, T., Guan, J. Z., Oyama, J., Higuchi, Y., & Makino, N. (2009). Age-related changes in subtelomeric methylation in the normal Japanese population. *J Gerontol A Biol Sci Med Sci, 64*, 426–434.

McGeer, P. L., Yasojima, K., & McGeer, E. G. (2001). Inflammation in Parkinson's disease. *Adv Neurol, 86*, 83–89.

Migliore L, Petrozzi L, Lucetti C, Gambaccini G, Bernardini S, Scarpato R, et al. (2002). Oxidative damage and cytogenetic analysis in leukocytes of Parkinson's disease patients. *Neurology, 58*, 1809–1815.

Okuda K, Khan MY, Skurnick J, Kimura M, Aviv H, Aviv A. (2000). Telomere attrition of the human abdominal aorta: Relationships with age and atherosclerosis. *Atherosclerosis*, 152, 391–398.

Panossian LA, Porter VR, Valenzuela HF, Zhu X, Reback E, Masterman D, et al. (2003). Telomere shortening in T cells correlates with Alzheimer's disease status. *Neurobiol Aging, 24*, 77–84.

Petrozzi L, Lucetti C, Gambaccini G, Bernardini S, Del Dotto P, Migliore L., et al. (2001). Cytogenetic analysis oxidative damage in lymphocytes of Parkinson's disease patients. *Neurol Sci, 22*, 83–84.

Turk, P. W., Laayoun, A., Smith, S. S., & Weitzman, S. A. (1995). DNA adduct 8-hydroxyl-2′-deoxyguanosine (8-hydroxyguanine) affects function of human DNA methyltransferase. *Carcinogenesis, 16*, 1253–1255.

Turk, P. W., & Weitzman, S. A. (1995). Free radical DNA adduct 8-OH-deoxyguanosine affects activity of HPA II

and MSP I restriction endonucleases. *Free Radic Res*, *23*, 255–258.

Uziel O, Singer JA, Danicek V, Sahar G, Berkov E, Luchansky M., et al. (2007). Telomere dynamics in arteries and mononuclear cells of diabetic patients: Effect of diabetes and of glycemic control. *Exp Gerontol*. *42*, 971–978.

Valdes AM, Andrew T, Gardner JP, Kimura M, Oelsner E, Cherkas LF., et al. (2005). Obesity, cigarette smoking, and telomere length in women. *Lancet*, *366*, 662–664.

Vaziri H, Schächter F, Uchida I, Wei L, Zhu X, Effros R., et al. (1993). Loss of telomeric DNA during aging of normal and trisomy 21 human lymphocytes, age groups. *Am J Hum Genet*, *52*, 661–667.

Vitte, J., Michel, B. F., Bongrand, P., & Gastaut, J. L. (2004). Oxidative stress level in circulating neutrophils is linked to neurodegenerative diseases. *J Clin Immunol*, *24*, 683–692.

Wachsman, J. T. (1997). DNA methylation and the association between genetic and epigenetic changes: Relation to carcinogenesis. *Mutat. Res*, *375*, 1–8.

Weitzman, S. A., Turk, P. W., Milkowski, D. H., & Kozlowski, K. (1994). Free radical adducts induce alterations in DNA cytosine methylation. *Proc Natl Acad Sci U S A*, *91*, 1261–1264.

Xiao, W., & Samson, L. (1993). In vivo evidence for endogenous DNA alkylation damage as a source of spontaneous mutation in eukaryotic cells. *Proc Natl Acad Sci U S A*, *90*, 2117–2121.

Yehezkel, S., Segev, Y., Viegas-Pe'quignot, E., Skorecki, K., & Selig, K. (2008). Hypomethylation of subtelomeric regions in ICF syndrome is associated with abnormally short telomeres and enhanced transcription from telomeric regions. *Hum Mol Genet*, *17*, 2776 – 2789.

Zakian, V. A. (1995). Telomeres: Beginning to understand the end. *Science*, *270*, 1601–1607.

ELSEVIER

Archives of Medical Research 43 (2012) 15–20

Archives of Medical Research

ORIGINAL ARTICLE

Alteration of Telomere Length and Subtelomeric Methylation in Human Endothelial Cell Under Different Levels of Hypoxia

Jing-Zhi Guan,[a,*] Wei-Ping Guan,[b,*] Toyoki Maeda,[c,*] and Naoki Makino[c]

[a]*The 309th Hospital of Chinese People's Liberation Army, Beijing, China*
[b]*Nanlou Neurology Department, Chinese People's Liberation Army General Hospital, Beijing, China*
[c]*Department of Cardiovascular and Geriatric Medicine, Kyushu University Beppu Hospital, Beppu, Oita, Japan*

Received for publication September 29, 2011; accepted January 18, 2012 (ARCMED-D-11-00475).

Background and Aims. Hypoxia-associated changes of telomeric structure in cell cultures have been analyzed mainly in cancer cells, stem cells, or cells transduced with vectors containing the telomerase gene, but not in somatic cells. The stability of telomere structure has been reported to be associated with subtelomeric methylation status. However, there are no reports of epigenetic alterations of telomeric regions of human somatic cells under hypoxia. This study aims at detecting and analyzing the subtelomeric methylation status in human somatic cells cultured under hypoxia.

Methods. Mean telomere length and telomerase activity of human umbilical vein endothelial cells (HUVECs) cultured in hypoxic conditions were measured. Subtelomeric methylation status of these cells was assessed by genomic Southern blot with telomere DNA probe using methylation-sensitive and -insensitive isoschizomers, *Msp*I and *Hpa*II.

Results. The telomerase activity in HUVECs correlated inversely with the oxygen concentration. Mild hypoxia (10 or 15% oxygen) increased the telomere lengths, whereas the telomere lengths did not appear to change when $<1\%$ O_2. The subtelomere of the shortest telomere range was methylated the most at 1% O_2.

Conclusions. Subtelomeric hypermethylation of short telomeres at 1% O_2 compared to milder hypoxia implied that the subtelomeric hypermethylation may yield telomere stability and favor the cell survival of short telomere-bearing cells. © 2012 IMSS. Published by Elsevier Inc.

Key Words: Hypoxia, Telomere, Subtelomere, DNA methylation, Telomerase, Endothelial cell.

Introduction

A telomere is a structure consisting of thousands of hexamer (TTAGGG/AATCCC) repeats and accessory peptide factors located at the termini of chromosomes TTAGGG (1,2). Telomere stability is maintained by telomerase, an RNA-directed DNA polymerase, as a template to add telomeric repeats onto chromosome ends (3). Hypoxia is a low oxygen stress condition where intracellular telomerase activity is elevated (4). In the previous publications describing hypoxia-associated changes of human telomerase activation in cell culture, cancer cells, stem cells, or cells transduced with vectors containing the telomerase gene were used, but not somatic cells. There are a limited number of previous reports describing the hypoxia-associated telomerase activation of human somatic cells. Endothelial cells have been regarded as an initial site of tissue injury by reactive oxygen during hypoxia (5). Hypoxia regulates cell growth and survival via modulating telomerase activity (6). Human umbilical vein endothelial cells (HUVECs) are human endothelial cells widely used in vascular research analyzing hypoxia-related changes, but there are a limited number of reports that address telomere length changes in vascular endothelial cells under hypoxia (7–9). In addition, there has been no study reported about the epigenetic change in telomeres under hypoxia. DNA methylation status, one of the genomic epigenetic conditions, in telomeric region has been reported to be altered in

*These authors equally contributed to this study.

Address reprint requests to: Toyoki Maeda, Department of Cardiovascular and Geriatric Medicine, The Kyushu University Beppu Hospital, 4546 Tsurumihara Beppu, Oita, 874-0838, Japan; Phone and Fax: +81-977-27-1681/1682; E-mail: maedat@beppu.kyushu-u.ac.jp

0188-4409/$ - see front matter.
doi: 10.1016/j.arcmed.2012.02.001

response to telomere length changes. A recent report showed that shortened telomere regions tend to accompany subtelomeric hypomethylation in fifth-generation mice, the telomerase activity-deficient *tert*$^{-}$/*tert*$^{-}$ mutant mouse (10). In humans, subtelomeric DNA is hypomethylated in sperm and ova, and these regions are subjected to de novo methylation during development (11,12). In humans this activity is carried out by DNMT3B (DNA methyltransferase 3B). Mutations in DNMT3B result in the autosomal-recessive ICF (immunodeficiency, centromeric region instability, facial anomalies) syndrome (13). Subtelomeres, neighboring regions to telomeres, in lymphoblastoid cells and fibroblast cells of ICF patients is hypomethylated to a similar extent as seen in sperm. Telomeres in this syndrome are also abnormally short (12). The aging process of somatic cells has been proposed to be associated with DNA damage caused by oxidative stress, and short telomeres with hypomethylated subtelomeres accumulate in the peripheral leukocytes with aging (14–16). Endothelial cells can also be a source of reactive oxygen species. Previous studies reported that oxidative stress shortens telomere lengths in cells cultured *in vitro* (17), and it has been identified as a key mediator of endothelial cell injury (18), which accelerated telomere attrition by oxidative DNA damage (17). In the present study we investigated the alterations in the telomere structural changes including the length shortening and subtelomeric methylation status and in telomerase activity under various levels of hypoxia to assess the effects of hypoxia on the telomere maintenance of human vascular endothelial cells.

Materials and Methods

Cell Culture

HUVECs were seeded at 3×10^5cells/ mL and cultured until about 80% confluence in a 5% CO_2 atmosphere at 37°C in complete endothelial cell basal medium-2 (EGM-2), which contained growth factors and was enriched with 2% fetal calf serum (Cambrex BioScience Walkersville, Walkersville, MD). Cells were then incubated for 5 days under hypoxic conditions (1, 10, 15% v/v O_2) and under normoxia (21% O_2). On the fifth day of culture, the DNA of cells was extracted by means of a DNA extraction kit (Qiagen, Valencia, CA), and the quality was assessed by 0.8% agarose gel electrophoresis. For hypoxic conditions, cells were cultured at 1%, 10% and 15% v/v O_2 in a modular incubator chamber (Billups-Rothenberg, San Diego, CA). The culture medium was changed every 24 h (2 mL/50 cm^2), and all experiments were performed using the cells after five passages. HUVECs were maintained under subconfluent conditions at all times. Cells were counted using a hemocytometer. Population doublings (PDs) were calculated using the formula:

$$PD = [\log(\text{expansion})/\log 2]$$

where expansion was the number of cells harvested divided by the initial number of cells seeded.

Telomere Detection

Telomere detection was performed as previously described (19–21). Briefly, aliquots of DNA (1 mg) were digested at 37°C with 3U *Msp* I or *Hpa* II for 2 h. The digests (20 mL) were electrophoresed and transferred to a positively charged nylon membrane (Roche Diagnostics, Mannheim, Germany) by the conventional Southern blotting method. Blotted membranes were hybridized to a 500-bp long (TTAGGG)n (n = 80–90) digoxigenin (dig)-labeled telomere probe. The membrane was then incubated with anti-digoxigenin-AP-specific antibody. The telomere probe was visualized by CSPD (provided with the kit). The membrane was then exposed to Fuji XR film with an intensifying screen. Autoradiogram smears were captured on an Image Master, and telomere length was assessed quantitatively.

Terminal Restriction Fragment (TRF) Analysis

The mean TRF was estimated using the formula:

$$\sum(\text{ODi} - \text{background})/\sum(\text{ODi} - \text{background/Li})(22)$$

where ODi is the chemiluminescent signal and Li is the length of the TRF fragment at position i. A loss of a few hundred base pairs from short telomeres is important to cellular ageing but may not be detected by traditional mean TRF analysis (21,23). In this study, therefore, we compared telomere length using telomere percentage analysis to detect minute changes of telomere length. This method has previously been used to determine the change of telomeres in rats (21). In brief, the intensity (photo-stimulated luminescence: PSL) was quantified as follows: each telomeric sample was divided into grid squares as follows according to the molecular size ranges: >9.4, 9.4–6.6, and <6.6 kb (Figure 1A). The percent of PSL in each molecular weight range was measured (% PSL = intensity of a defined region-background × 100/total lane intensity-background). Telomeric methylation was assessed by comparing the *Msp*I telomere length distribution and that of *Hpa*II. The difference between the percent of *Msp*I PSL (%*Msp*I-TRF) and the *Hpa*II PSL (%*Hpa*II-TRF) in each molecular weight range was calculated (Figure 1B).

Telomerase Activity Assay

Telomerase activity was measured using the TRAP-eze Telomerase Detection Kit according to the manufacturer's protocol (Intergen, Purchase, NY). Relative telomerase activity was calculated, as the value measured at 21% O_2 was put as 1.0 at each experiment set.

Statistical Analysis

The normality of the data was examined with the Kolmogorov-Smirnov test, and homogeneity of variance

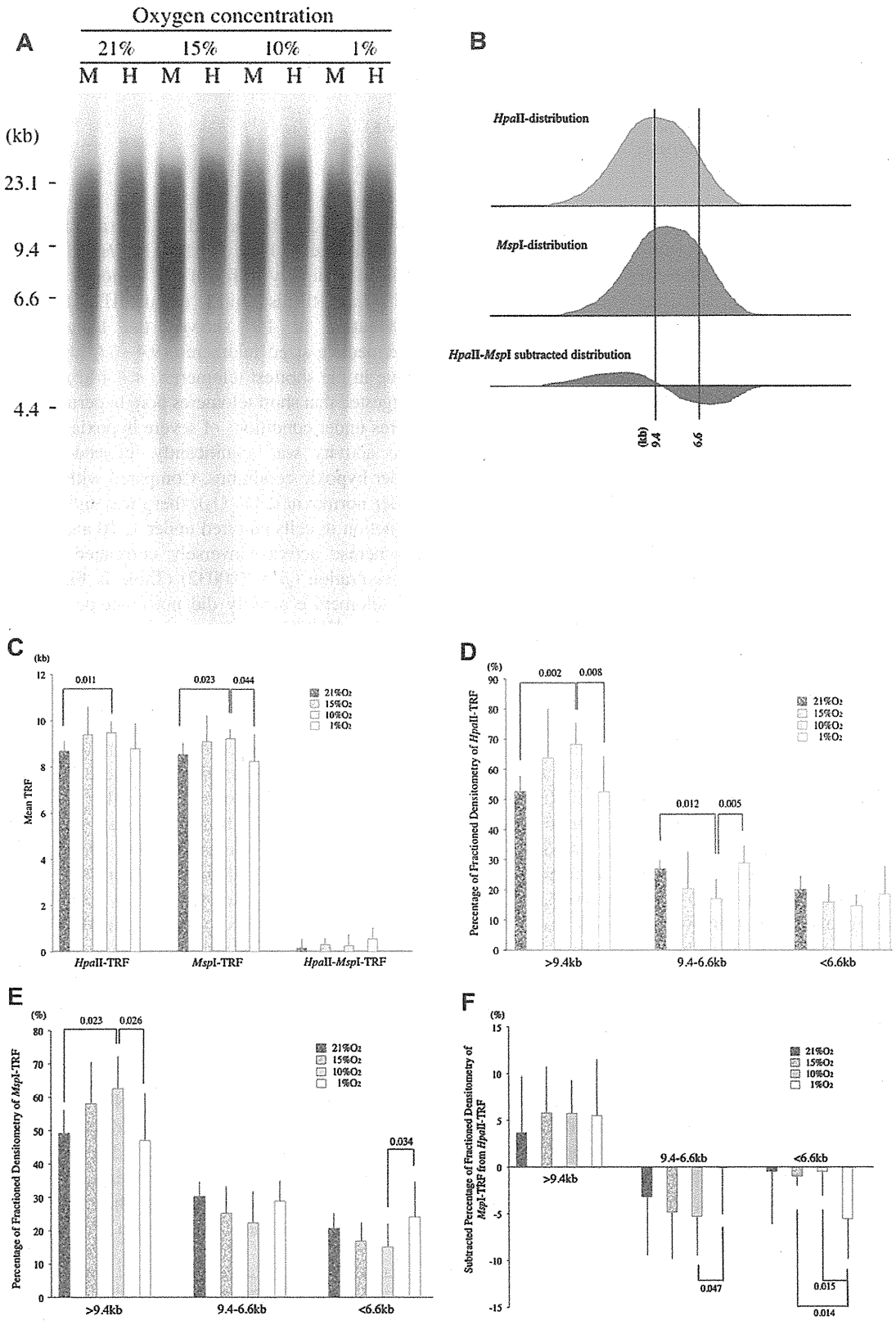

Figure 1. Analysis of the terminal restriction fragment length (TRF) by the methylation sensitive- (*Hpa*II) and -insensitive (*Msp*I) isoschizomeric restriction enzymes. (A) Representative genomic Southern blot probed with telomere DNA of human umbilical vein endothelial cells (HUVECs) at different oxygen concentrations. M: *Msp*I digest, H: *Hpa*II digest. (B) Schema of the densitometries of genomic Southern blot digested with *Hpa*II, *Ms*I and *(continued on next page)*

Table 1. Population doublings of HUVECs at different oxygen levels

Oxygen concentration (%)	1	10	15	21
Population doublings	4.61 ± 0.07***	4.47 ± 0.11***	3.82 ± 0.35	3.94 ± 0.29

HUVECs, human umbilical vein endothelial cells.
The starting cell count at day 0 was 3 x 10^5/mm^3. Cell numbers were counted at day 5.
Data are expressed as mean ± standard deviation.
***p <0.001 vs. 21% oxygen.

with Levene median test. If both normally distributed and equal variance tests were passed, the differences in telomeres length including mean TRF length and telomeres percentage analysis were studied using one-way ANOVA test followed by all pairwise multiple comparison procedures using Tukey's post-hoc test. If the data did not show normality or equal variance, logarithmic or square-root transformations were used to normalize the data for fitting one-way ANOVA. Data are expressed as mean ± standard deviation for five replicate experiments; p <0.05 was accepted as statistically significant. The linear regression model was used to assess the correlation between the hypoxia level and telomerase activity. All analyses were carried out using Sigma Statistical Analysis Software (Sigma 2.03, 2001; Sigma, St. Louis, MO).

Results

Population doublings were determined after 5-day culture at different oxygen concentrations. Lower oxygen (1 and 10%) yielded significantly larger cell numbers than for 21% O_2 (Table 1). Lower oxygen seemed to provide a growth advantage to vascular endothelial cells. The mean TRF lengths were determined in HUVECs under the different conditions. Telomeres were longer at 10% O_2 than under normoxia in both *Msp*I and *Hpa*II digests (Figures 1A, 1C). Telomere length distribution is shown in Figures 1D-F. We observed a significant increase for the longest *Msp*I-TRF (>9.4 kb) at 10% O_2. In addition, a decrease of the long telomeres (>9.4 kb) and an increase of the shortest telomeres (<6.6 kb) were observed at 1% O_2, compared to 10% O_2 (Figure 1E). These observations suggested that telomeres were elongated under mild hypoxia such as at 10% O_2, and that the telomere-elongating effect of hypoxia was lost under conditions of severe hypoxia, such as at 1% O_2. On the other hand, the subtracted *Hpa*II-*Msp*I TRF was not significantly different among the different hypoxic conditions, although a subtle tendency toward an increase in subtelomeric methylation appeared at 1% O_2 (Figure 1A, 1C). To assess the methylation status of subtelomeres under hypoxia in greater detail, the *Hpa*II-TRF-distribution and the subtracted *Hpa*II-*Msp*I TRF were analyzed (Figures 1D–1F). *Hpa*II-TRF distribution showed a slightly different but a mostly similar pattern to the *Msp*I-TRF distribution (Figure 1D, 1E). The subtracted distribution at 1% showed the lowest value in the intermediate-sized telomeres (9.4–6.6 kb) and the highest value in the shortest telomeres (<4.4 kb) (Figure 1F). This suggested that short telomeres bore hypermethylated subtelomeres under conditions of severe hypoxia (1% O_2). Telomerase activity was significantly induced in cells cultured under hypoxic conditions. Compared with the cells cultured under normoxia (21% O_2), there was significant telomerase induction in cells cultured under 1, 10 and 15% O_2, and the telomerase activity inversely correlated with the oxygen concentration (p = 0.0032) (Table 2, Figure 2). However, the telomerase activity did not coincide with the telomere length of HUVECs under severe hypoxia (1% O_2).

Discussion

A recent report showed that the immune cells bear higher telomerase activity, as their telomere lengths are longer (24). This observation implies that other cell types, including HUVECs, bearing longer telomeres may also express higher telomerase activity. In the present study, HUVECs restored telomerase expression under hypoxic conditions. The elevated telomerase activity under hypoxia would cause telomeres to elongate in HUVECs. The elevation of telomerase in normal primary human diploid lung fibroblasts (PHLF) is detected after a 24-h culture under hypoxia (1.5% O_2) (25). Similarly, the vascular smooth muscle cell telomerase activity is induced at 6 h after exposure of the cultures to 1% O_2 (6). From these observations, it can be concluded that hypoxia activates telomerase in various kinds of human somatic cells with a similar mechanism within several hours. In addition, our observations showed that modest hypoxic conditions such as 10 and 15% O_2 could also activate telomerase in human vascular endothelial cells, suggesting that the mechanism functions in response to the level of hypoxia. Telomerase activity is

the subtracted *Hpa*II-*Msp*I densitometric telomere length distribution. (C) Mean *Msp*I-, *Hpa*II-, and the subtracted *Hpa*II-*Msp*I-TRFs under different oxygen levels are presented. (D–F) Densitometry of each telomere smear of Southern blot is divided into three regions according to molecular weight markers (>9.4, 9.4–6.6, <6.6 kb). *Hpa*II-TRF distribution (D), *Msp*I-TRF distribution (E) and the subtracted *Hpa*II-*Msp*I-TRF distribution (F) (D–E = F) in HUVECs cultured under different levels of hypoxia. Data are expressed as mean ± standard deviation. The standard deviation is depicted as a horizontal bar on each of the mean columns. Numbers represent p values for the indicated comparisons.

Table 2. Relative telomerase activity in HUVECs cultured under different levels of hypoxia

Oxygen concentration (%)	1	10	15	21
Relative telomerase activity	5.8 ± 0.6***	2.9 ± 0.4**	2.1 ± 0.5*	1

HUVECs, human umbilical vein endothelial cells.
Data are expressed as mean ± standard deviation.
*p <0.05.
**p <0.01.
***p <0.001 vs. 21% oxygen.

an important factor in cell proliferation, and hypoxia exposure has been shown to increase hTERT gene expression, suggesting that telomerase activation may also be a mechanism that protects against genetic stress induced by hypoxia (6,26). However, the TRF change and the elevated telomerase activity of HUVECs under hypoxia did not correlate at 1% O_2. This result differs from the formerly reported results in cases of human vascular smooth muscle cells and mouse fibroblasts (6,27). Vascular endothelial cells may be less able to tolerate severe hypoxia than other types of cell. The growth rate and telomere length stability of an individual cell under hypoxia all depend on the balance among various cellular mechanisms.

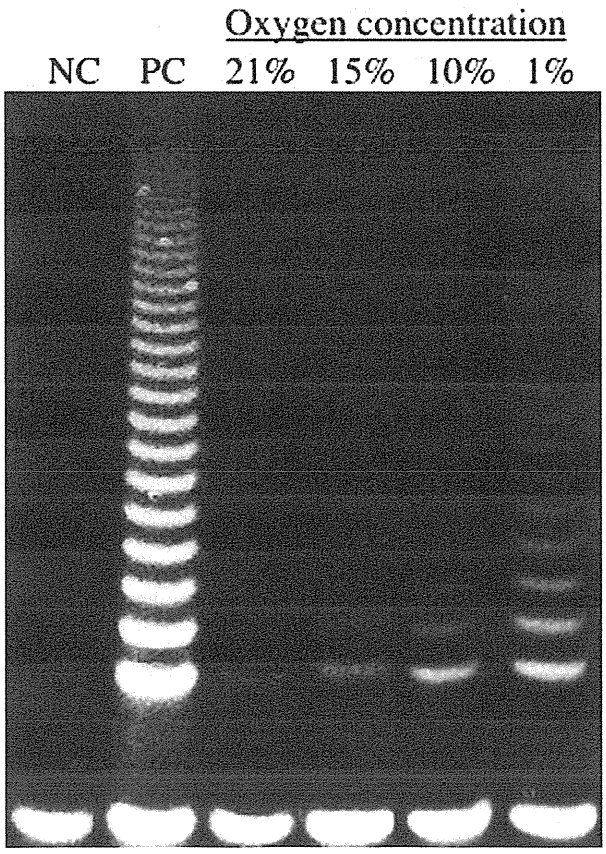

Figure 2. Telomerase activity of HUVECs at different oxygen concentrations. The photograph of a representative TRAP assay result for HUVECs at different oxygen concentrations is presented. The materials used for the positive control (PC) and negative control (NC) were provided with the kit.

Severe hypoxia-associated genotoxic effects may counteract the telomere-elongating effects yielded by lowered oxidative stress in HUVECs under extremely low oxygenic conditions. We found a tendency for an increase in the proportion of the longest telomeres (>9.4 kb) under mild hypoxia at 10% O_2, accompanied by elongation of the mean telomere length, and the tendency was lost under severe hypoxic condition at 1% O_2. Thus, the telomere-elongating effect disappeared under severe hypoxia at 1% O_2 such that the telomere length and its distribution seemed to be similar between 21% O_2 and 1% O_2. However, the subtelomeric methylation status of short telomeres was different under these conditions. The growth activity and the telomerase activity were elevated even at 1% O_2, similar to when cells were cultured under milder hypoxia (10–15% O_2), whereas the mean telomere length shortened and subtelomeric methylation of short telomeres was elevated at 1% O_2. Telomerase activation has been reported to be related to growth activity, telomere elongation and enhanced subtelomeric methylation (3,10,28). However, telomeres were not elongated at 1% O_2 with all of the other phenotypes. In addition, the subtelomeric methylation did not increase under mild hypoxic conditions, in spite of the elevated telomerase activity. Subtelomeric hypermethylation in short telomeres seemed to coincide with the disappearance of the hypoxia-associated telomere shortening effect. This elevation of the subtelomeric methylation may be associated with a growth advantage under severe hypoxia, even though the telomere elongation by enhanced telomerase activity was no longer present. As a result, HUVECs bearing high telomerase activity and hypermethylated subtelomeres of the short telomeres may have a selective growth advantage at 1% O_2. Hypermethylation of the subtelomeres of short telomeres may be one of the protective mechanisms for the telomere structure. The ICF syndrome, which results from a deficiency in a DNA methyltransferase, results in abnormally short telomeres with hypomethylated subtelomeres (12), indicating that subtelomeric methylation functions to protect telomeres from attrition. Although neither the activated telomerase nor the subtelomeric hypermethylation seemed to elongate the telomere length sufficiently under severe hypoxic conditions, the elevated methylation of subtelomere in short telomeres may prevent the neighboring telomere from experiencing excessive shortening. Hypermethylation of subtelomeres in short telomeres is therefore a possible

candidate indicator of the growth advantage of somatic cells under conditions yielding the acceleration of telomere attrition.

In summary, a limited range of hypoxia yielded telomere elongation of HUVECs. Although telomerase activity was highest, severe hypoxia at 1% O_2 yielded no telomere elongation. This discrepancy has not been observed in other cell types. Previous studies and the present study imply that the determinants of telomere length under severe hypoxia may vary among different cell types. Alterations in the subtelomeric methylation of cultured cells were first identified under severe hypoxia. Our study is a pivotal step that clarifies the biological significance of subtelomeric methylation under hypoxia. The observed hypermethylation appeared to have a protective effect for the telomere structure in cells bearing short telomeres with active cell growth and with activated telomerase, that were exposed to telomere-shortening conditions, such as severe hypoxia. Further study is therefore necessary to fully elucidate the mechanism of tolerance to severe hypoxia in regard to the telomere stability of vascular endothelial cells.

Acknowledgments

This work was supported, in part, by the National Natural Science Fund (NSFC) (81170329/H2501) and by a Grant-in-Aid from the Ministry of Education, Science, and Culture of Japan (#23590885).

References

1. Blackburn EH. Structure and function of telomeres. Nature 1991;350: 569–573.
2. Zakian VA. Telomeres: beginning to understand the end. Science 1995;270:1601–1607.
3. Greider CW. Telomere length regulation. Annu Rev Biochem 1996;65: 337–365.
4. Napier CE, Veas LA, Kan CY, et al. Mild hyperoxia limits hTR levels, telomerase activity, and telomere length maintenance in hTERT-transduced bone marrow endothelial cells. Biochim Biophys Acta 2010;1803:1142–1153.
5. Ratych RE, Chuknyiska RS, Bulkley GB. The primary localization of free radical generation after anoxia/reoxygenation in isolated endothelial cells. Surgery 1987;102:122–131.
6. Minamino T, Mitsialis SA, Kourembanas S. Hypoxia extends the life span of vascular smooth muscle cells through telomerase activation. Mol Cell Biol 2001;21:3336–3342.
7. Zweier JL, Kuppusamy P, Thompson-Gorman S, Klunk D, Lutty GA. Measurement and characterization of free radical generation in reoxygenated human endothelial cells. Am J Physiol 1994;266:C700–C708.
8. Hastings R, Qureshi M, Verma R, Lacy PS, Williams B. Telomere attrition and accumulation of senescent cells in cultured human endothelial cells. Cell Prolif 2004;37:317–324.
9. Zhang J, Hui C, Su L, Xiaoyun W, Xi H, Yingchuan F. The association between telomere length and sensitivity to apoptosis of HUVEC. Adv Exp Med Biol 2010;664:47–53.
10. Benetti R, García-Cao M, Blasco MA. Telomere length regulates the epigenetic status of mammalian telomeres and subtelomeres. Nat Genet 2007;39:243–250.
11. Brock GJ, Charlton J, Bird A. Densely methylated sequences that are preferentially localized at telomere-proximal regions of human chromosomes. Gene 1999;240:269–277.
12. Yehezkel S, Segev Y, Viegas-Péquignot E, et al. Hypomethylation of subtelomeric regions in ICF syndrome is associated with abnormally short telomeres and enhanced transcription from telomeric regions. Hum Mol Genet 2008;17:2776–2789.
13. Hansen RS, Wijmenga C, Luo P, et al. The DNMT3B DNA methyltransferase gene is mutated in the ICF immunodeficiency syndrome. Proc Natl Acad Sci USA 1999;96:14412–14417.
14. Maeda T, Guan JZ, Oyama J, et al. Age-related changes in subtelomeric methylation in the normal Japanese population. J Gerontol A Biol Sci Med Sci 2009;64:426–434.
15. Maeda T, Guan JZ, Higuchi Y, Oyama J, Makino N. Age-related alterations in subtelomeric methylation in sarcoidosis patients. J Gerontol A Biol Sci Med Sci 2009;64:752–760.
16. Maeda T, Guan JZ, Oyama J, Higuchi Y, et al. Aging-associated alteration in subtelomeric methylation in Parkinson's disease. J Gerontol A Biol Sci Med Sci 2009;64:949–955.
17. von Zglinicki T. Oxidative stress shortens telomeres. Trends Biochem Sci 2002;27:339–344.
18. Taniyama Y, Griendling KK. Reactive oxygen species in the vasculature: molecular and cellular mechanisms. Hypertension 2003;42:1075–1081.
19. Harley CB, Futcher AB, Greider CW. Telomeres shorten during ageing of human fibroblasts. Nature 1990;345:458–460.
20. Vaziri H, Dragowska W, Allsopp RC, et al. Evidence for a mitotic clock in human hematopoietic stem cells: loss of telomeirc DNA with age. Proc Natl Acad Aci USA 1994;91:9857–9860.
21. Cherif H, Tarry JL, Ozanne SE, et al. Ageing and telomeres: a study into organ- and gender-specific telomere shortening. Nucl Acid Res 2003;31:1576–1583.
22. de Lange T, Shiue L, Myers RM, et al. Structure and variability of human chromosome ends. Mol Cell Biol 1990;10:518–527.
23. Hemann MT, Strong MA, Hao LY, et al. The shortest telomere, not average telomere length, is critical for cell viability and chromosome stability. Cell 2001;107:67–77.
24. Lin J, Epel E, Cheon J, et al. Analyses and comparisons of telomerase activity and telomere length in human T and B cells: insights for epidemiology of telomere maintenance. J Immunol Methods 2010; 352:71–80.
25. Bell EL, Klimova TA, Eisenbart J, et al. Mitochondrial reactive oxygen species trigger hypoxia-inducible factor-dependent extension of the replicative life span during hypoxia. Mol Cell Biol 2007;27: 5737–5745.
26. Seimiya H, Tanji M, Oh-hara T, et al. Hypoxia up-regulates telomerase activity via mitogen-activated protein kinase signaling in human solid tumor cells. Biochem Biophys Res Commun 1999;260:365–370.
27. Nishi H, Nakada T, Kyo S, et al. Hypoxia-inducible factor 1 mediates upregulation of telomerase (hTERT). Mol Cell Biol 2004;24: 6076–6083.
28. Geserick C, Tejera A, González-Suárez E, Klatt P, Blasco MA. Expression of mTert in primary murine cells links the growth-promoting effects of telomerase to transforming growth factor-beta signaling. Oncogene 2006;25:4310–4319.

Clinical Investigations

Continuous Positive Airway Pressure Therapy Improves Vascular Dysfunction and Decreases Oxidative Stress in Patients With the Metabolic Syndrome and Obstructive Sleep Apnea Syndrome

Address for correspondence:
Jun-ichi Oyama, MD
Department of Cardiovascular, Respiratory and Geriatric Medicine
Kyushu University Hospital at Beppu and Medical Institute of Bioregulation
Kyushu University
4546 Tsurumihara, Beppu, Oita, 874-0838, Japan
joyama@tsurumi.beppu.kyushu-u.ac.jp

Jun-ichi Oyama, MD; Hiroaki Yamamoto, MD; Toyoki Maeda, MD; Akira Ito, MD; Koichi Node, MD; Naoki Makino, MD

Department of Cardiovascular, Respiratory, and Geriatric Medicine (Oyama, Maeda, Makino), Kyushu University Hospital at Beppu and Medical Institute of Bioregulation, Kyushu University, Oita, Japan; Department of Cardiovascular Medicine (Oyama, Node), Saga University, Saga, Japan; Gakkentoshi Clinic (Yamamoto, Ito), Fukuoka, Japan

ABSTRACT

Background: Patients with obstructive sleep apnea syndrome (OSAS) are always exposed to intermittent hypoxia and reoxygenation. The metabolic syndrome (MetS) and OSAS are also known to accelerate atherosclerosis, diabetes, and dyslipidemia. Therefore, nasal continuous positive airway pressure (CPAP) therapy may have beneficial effects in patients with the MetS and OSAS.

Hypothesis: This study in patients with the MetS and OSAS tested the validity of the hypothesis that chronic CPAP therapy improves factors involved in atherosclerosis, including impaired endothelial function.

Methods: Thirty-two patients (19 males and 13 females, mean age 54 ± 9 y) diagnosed with the MetS and OSAS were enrolled in the study and received CPAP therapy for 3 months. Vascular function was investigated by measuring forearm blood flow (FBF) responses to reactive hyperemia (RH) using venous occlusion strain-gauge plethysmography. Biochemical markers were also measured before and after this procedure.

Results: Basal apnea-hypopnea index was statistically correlated with FBF response to RH. The FBF response to RH was increased significantly after 3 months of CPAP therapy. A significant increase in plasma nitric oxide levels and a decrease in the levels of asymmetrical dimethylarginine, thiobarbituric acid reactive substance, soluble Fas ligand, and soluble CD40 ligand were detected after CPAP therapy. The plasma concentrations of tumor necrosis factor-α, interleukin (IL)-6, and IL-8 also decreased significantly with CPAP therapy, whereas IL-1β levels remained unchanged.

Conclusions: Continuous positive airway pressure therapy has beneficial effects on vascular function and inflammatory and oxidative stress in patients with the MetS and OSAS.

Introduction

The metabolic syndrome (MetS) is characterized by a clustering of metabolic abnormalities, including obesity, hyperglycemia, dyslipidemia, and hypertension. The syndrome has been identified as a common precursor to the development of cardiovascular (CV) disease.[1] The prevalence of the MetS is increasing in Japan as a result of changes in diet and physical activity during recent decades.[2] This has resulted in an urgent need to obtain appropriate evidence for treatment of individuals with the MetS who have a high risk of developing CV disease, thereby preventing a further increase in the incidence of the syndrome.

Obstructive sleep apnea syndrome (OSAS) is also a highly prevalent disorder, affecting approximately 17% of adults,[3] and is associated with repetitive episodes of transient oxygen desaturation that cause apneas and hypopneas during sleep. The syndrome is regarded as an independent risk factor for a number of CV diseases, including systemic arterial hypertension,[4,5] coronary artery disease, congestive cardiac failure, and cerebral vascular events.[4,6] Treatment with nasal continuous positive airway pressure (CPAP) ameliorates oxygen desaturation and decreases CV morbidity[7] and mortality.[8,9] Although the pathophysiological basis of CV complications in OSAS is multifactorial, involving sympathetic excitation, endothelial dysfunction, inflammation, and insulin resistance,[10] it is likely that the intermittent episodes of hypoxia, particularly the associated episodes of intermittent reoxygenation, are important mediators of these complications. Therefore,

The authors have no funding, financial relationships, or conflicts of interest to disclose.

Received: August 18, 2011
Accepted with revision: October 30, 2011

Published online in Wiley Online Library (wileyonlinelibrary.com)
DOI:10.1002/clc.21010

patients who suffer from not only the MetS, but also OSAS, must be treated appropriately. However, the effects of CPAP therapy on endothelial dysfunction and atherosclerotic biomarkers are not fully understood.

Methods

Study Design and Protocol

The Institutional Review Board of Human Research at Kyushu University approved this study, and written, informed consent was obtained from all participants. The study was a single-arm prospective design that examined the impact of CPAP treatment on endothelial function and biochemical alterations, including inflammation and oxidative stress, in patients with the MetS and stable OSAS (apnea-hypopnea index [AHI] >20 events/h).

Patients with the MetS suspected of having OSAS were recruited. Patients with a history of heart failure, severe coronary artery disease with residual cardiac ischemia or arrhythmia, significant pulmonary disease, or subjects taking β-blockers or other negative chronotropic drugs were excluded. Patients already diagnosed as having hyperglycemia, dyslipidemia, and/or hypertension and who were receiving drug treatment and satisfied the criteria of the MetS were included the study.

At the start of the study, 53 patients with the MetS agreed to participate and underwent full polysomnography, and 40 newly diagnosed candidates for CPAP therapy who had an AHI >20 events per hour were enrolled. All the patients were requested to fast and underwent polysomnography, followed by blood sampling and endothelial function tests between 9 and 11 A.M. They were assessed using the Epworth Sleepiness Scale (ESS) to investigate changes in subjective daytime sleepiness.[11] Five patients were excluded because they withdrew from participation, 1 patient stopped CPAP therapy, and 2 patients were excluded due to poor compliance (<60%). The remaining 32 patients with the MetS and OSAS who received CPAP therapy were evaluated throughout the study. No patient changed their medications during the study. All the experimental evaluations were repeated 3 months after CPAP intervention in all the patients.

Definition of MetS

The MetS was defined according to the Japanese criteria as the presence of ≥2 abnormalities in addition to a waist circumference >85 cm in males and >90 cm in females. Other abnormalities included in the definition were (1) dyslipidemia, indicated by hypertriglyceridemia (serum triglyceride concentration ≥150 mg/dL) and/or low high-density lipoprotein cholesterol (serum concentration ≤40 mg/dL); (2) hypertension, indicated by systolic blood pressure ≥130 mm Hg and/or diastolic blood pressure ≥85 mm Hg; and (3) high fasting glucose, indicated by serum glucose concentration ≥110 mg/dL.

Polysomnography and Definition of Obstructive Sleep Apnea Syndrome

Full polysomnography was performed using the Somno Track Pro system (Fukuda Denshi Co, Ltd, Tokyo, Japan). An electroencephalograph (EEG), electro-oculography, electromyography, and electrocardiogram were performed simultaneously. Surface electrodes were used to record 2 channels of the EEG (CA2, C4A1), right and left electro-oculography, and submental electromyography. Respiratory movements of the chest and abdomen were monitored by inductive plethysmography bands, and nasal pressure cannulas were used to record airflow. Arterial oxygen saturation ($SatO_2$) was measured using fingertip pulse oximeters. Apnea was defined as complete cessation of airflow for ≥10 seconds, and hypopnea as a reduction in airflow of ≥50%, accompanied by ≥4% oxygen desaturation, or an EEG arousal from sleep. Apnea-hypopnea index was defined as the total number of apneas and hypopneas per hour of sleep. The patients who had an AHI >20 were enrolled in this study as candidates for CPAP therapy.

CPAP Therapy

Patients with an AHI >20 slept while attached to the automatic titration device (ResMed S8; ResMed Ltd, Sydney, Australia). After using the CPAP device for ≥3 months, data of CPAP usage and mean AHI were obtained from data cards inside the CPAP machine. Compliance with CPAP was defined as percent of days with CPAP usage for ≥4 hours among the total days of the study. Subjects who showed good compliance (≥60%) with the CPAP device were included in the analysis. Sleep stages and respiratory parameters were scored according to the standard criteria of the American Academy of Sleep Medicine.[12] At the end of study protocol, the patients had a repeat polysomnography while using CPAP devices to evaluate the exact evaluation of the efficacy of CPAP therapy.

Measurement of Forearm Blood Flow

The measurement of FBF has been described previously.[13] Briefly, all the studies were performed in a temperature-controlled room, with the subjects in the resting and supine states. Forearm blood flow ($mL \cdot min^{-1} \cdot 100\ mL^{-1}$ of forearm volume) was measured by the venous-occlusion technique using a mercury-filled silastic strain-gauge plethysmograph (model EC-5R; D.E. Hokanson Inc, Bellevue, WA). The subjects were requested to rest for 20 minutes to obtain stable baseline measurements. After the baseline condition was established, the basal FBF measurement was obtained from the rate of the increase in forearm volume, with venous return from the forearm being prevented by inflation of a cuff on the upper arm using a venous occlusion pressure of 50 mm Hg. The flow measurements were recorded for 7 seconds every 15 seconds, and the mean of 4 measurements was used in the analyses. To evaluate FBF induced by reactive hyperemia (RH), FBF was occluded by inflation of a cuff placed over the left upper arm to a pressure of 200 mm Hg for 5 minutes. After the ischemic cuff occlusion was released, FBF was measured every 15 seconds for 3 minutes, according to the procedures described above.

Biochemical Analyses

Blood samples were collected from the patients before the FBF measurements, centrifuged at 4°C within 20

Published online in Wiley Online Library (wileyonlinelibrary.com)
DOI:10.1002/clc.21010

minutes, and then stored at −80°C until assayed. The plasma levels of the nitric oxide compounds (NOx; $NO2^-$+ $NO3^-$) and asymmetrical dimethylarginine (ADMA) were measured by high-performance liquid chromatography using methods described previously.[14] The plasma levels of tumor necrosis factor-α (TNF-α), interleukin 1β (IL-1β), IL-6, IL-8 (BioSource International, Inc, Camarillo, CA), thiobarbituric acid reactive substance (TBARS; Cayman Chemical Co, Ann Arbor, MI), soluble CD40 ligand (sCD40L; BioSource International), and soluble Fas ligand (sFasL; Medical Biological Laboratories Co, Ltd, Nagoya, Japan) were measured by enzyme-linked immunosorbent assay.[13,14] The biochemical parameters were measured in duplicate and the mean value used in the analyses.

Statistical Analysis

The data were expressed as mean ± SD. Paired *t* tests were performed to compare endothelial responses or biochemical changes before and after CPAP intervention. A univariate regression analysis was carried out to evaluate the correlations of AHI and various parameters, including FBF response to RH at baseline. To assess independent determinants that showed significant correlations with improvement of FBF to RH, multivariate analysis based on stepwise regression analysis used after a univariate regression analysis was carried out as the independent variable. The odds ratios and 95% confidence intervals were calculated. A P value of <0.05 was considered statistically significant.

Results

Patient Characteristics and Effect of Continuous Positive Airway Pressure on Physiological Factors and Sleep Status

The baseline characteristics of the 32 patients with OSAS are presented in Table 1. Mean AHI before treatment was 56.2 ± 21.6, and mean ESS score at baseline was 17.4 ± 5.3. Continuous positive airway pressure therapy markedly improved AHI and ESS score. Waist circumference, body weight, body mass index, and arterial blood pressure were decreased significantly after treatment with CPAP, in association with a slight improvement in hyperglycemia and dyslipidemia. However, glycated hemoglobin (HbA_{1c}) did not alter after CPAP therapy; HbA_{1c} reflects the glycemic profile over a period of a few months prior to the measurement. Therefore, longer observation may be needed.

Association Between Apnea-Hypopnea Index and Forearm Blood Flow Responses to Reactive Hyperemia Before Treatment

There was a significant inverse correlation between the level of basal AHI and the FBF responses to RH (Figure 1; $r = 0.569$, $P = 0.0007$). The basal AHI also correlated with the levels of NOx ($r = 0.628$, $P = 0.0001$), ADMA ($r = 0.494$, $P = 0.004$), TBARS ($r = 0.462$, $P = 0.008$), CD40L ($r = 0.356$, $P = 0.046$), and TNF-α ($r = 0.420$, $P = 0.017$). The FBF response to RH has significant associations with the levels of NOx ($r = 0.559$, $P = 0.0009$), ADMA ($r = 0.436$, $P = 0.0127$), and TBARS ($r = 0.435$, $P = 0.0128$).

Table 1. Baseline Characteristics and Changes in Physiological Parameters of the Patients Following CPAP Therapy

	Before CPAP Therapy	After CPAP Therapy	*P* Value
Age, y	53.9 ± 8.6		
Gender, M/F	19/13		
Height, cm	164.3 ± 8.6		
Weight, kg	72.6 ± 13.0	71.1 ± 11.5	<0.01
BMI, kg/m²	26.7 ± 3.6	26.2 ± 3.3	<0.01
Waist circumference, cm	90.7 ± 6.5	90.2 ± 6.5	<0.01
ESS	17.4 ± 5.3	7.2 ± 3.9	<0.01
AHI, events/h	56.2 ± 21.6	3.5 ± 2.3	<0.01
Hypertension, n (%)	26 (81.3%)		
Receiving drug, n (%)	11 (42.3%)		
SBP, mm Hg	142.5 ± 11.0	137.7 ± 7.9	<0.01
DBP, mm Hg	80.2 ± 8.3	76.3 ± 6.0	<0.01
mBP, mm Hg	101.0 ± 8.1	96.8 ± 5.7	<0.01
HR, bpm	73.9 ± 8.1	73.3 ± 7.6	0.71
DM, n (%)	22 (71.0)		
Receiving drug, n (%)	11 (50.0)		
FBG, mg/dL	113.9 ± 6.5	110.7 ± 7.1	0.032
HbA_{1c}, %	5.9 ± 0.4	5.9 ± 0.4	0.28
Dyslipidemia, n (%)	26 (81.3)		
Receiving drug, n (%)	8 (30.8)		
LDL-C, mg/dL	128.4 ± 25.6	123.3 ± 16.1	0.090
HDL-C, mg/dL	45.0 ± 9.4	47.1 ± 7.0	0.070
Triglycerides, mg/dL	220.4 ± 36.9	215.1 ± 36.8	0.305

Abbreviations: AHI, apnea-hypopnea index; BMI, body mass index; CPAP, continuous positive airway pressure; DBP, diastolic blood pressure; DM, diabetes mellitus; ESS, Epworth Sleepiness Scale; F, female; FBG, fasting blood glucose; HDL-C, high-density lipoprotein cholesterol; HR, heart rate; LDL-C, low-density lipoprotein cholesterol; M, male; mBP, mean blood pressure; SBP, systolic blood pressure.

Effect of Continuous Positive Airway Pressure on Forearm Blood Flow Responses to Reactive Hyperemia

Baseline FBFs were almost the same before and after CPAP treatment. As shown in Figure 2, the peak FBF RH-induced response was increased significantly after CPAP treatment.

Assessment of Biochemical Changes Associated With the Use of Continuous Positive Airway Pressure

After CPAP therapy, the level of NOx increased, whereas the levels of TBARS, ADMA, sFasL, and sCD40L decreased (Figure 3). Decreased plasma levels of TNF-α, IL-6, and IL-8 were also observed after CPAP treatment, although the level of IL-1β remained unchanged (Figure 4). Table 2 shows the

Published online in Wiley Online Library (wileyonlinelibrary.com)
DOI:10.1002/clc.21010

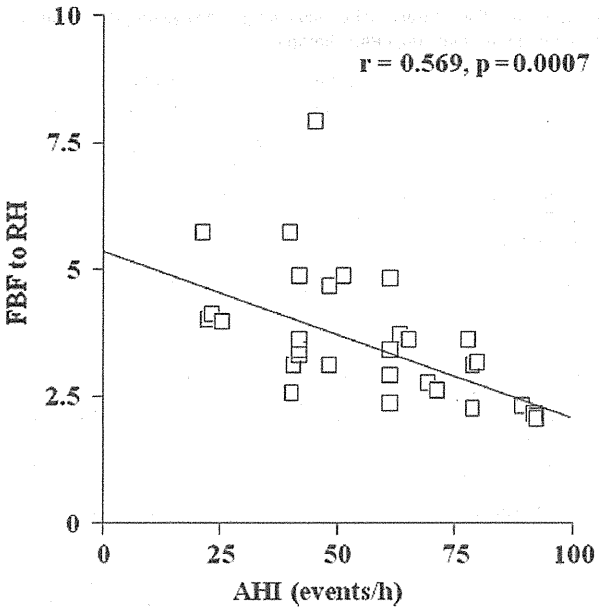

Figure 1. The correlation between AHI and FBF response to RH. Abbreviations: AHI, apnea-hypopnea index; FBF, forearm blood flow; h, hour; RH, reactive hyperemia.

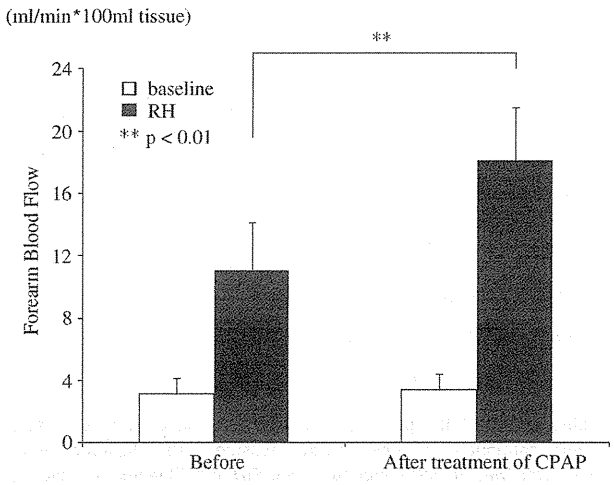

Figure 2. The effects of CPAP therapy on endothelial function in patients with MetS and OSAS for 3 months. Abbreviations: CPAP, continuous positive airway pressure; MetS, metabolic syndrome; OSAS, obstructive sleep apnea syndrome; RH, reactive hyperemia. $^{**}P < 0.01$.

results of multiple stepwise regression analysis to find the determinants of improvement of FBF response to RH. The independent variables were increment of NOx, decrement of ADMA, IL-6, and TNF-α.

Discussion

The present study demonstrated that medium-term CPAP treatment ameliorated RH-induced FBF responses in patients with the MetS and OSAS. We also showed that CPAP therapy markedly reduced the plasma levels of TBARS, TNF-α, IL-6, IL-8, sFas L, and sCD40L. Continuous positive airway pressure therapy resulted in an improvement

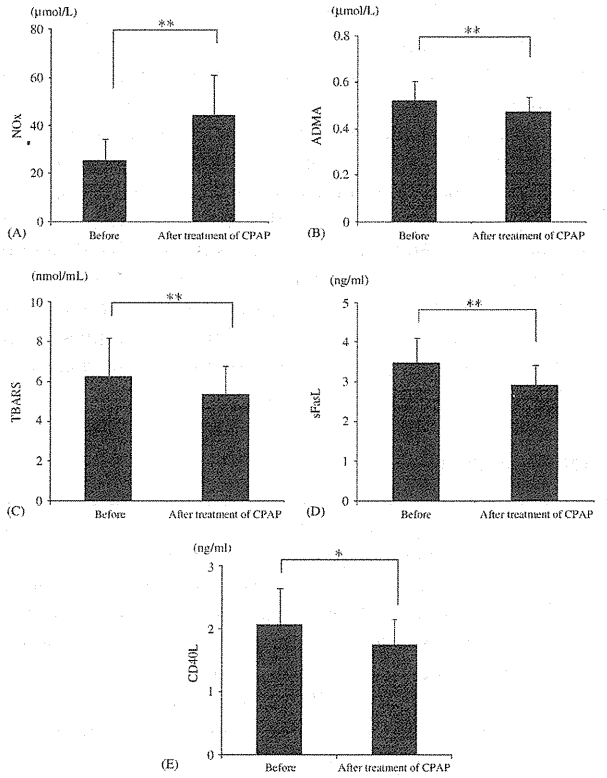

Figure 3. Alterations in the plasma levels of NOx (A), ADMA (B), TBARS (C), sFasL (D), and CD40L (E) in each group. Abbreviations: ADMA, asymmetrical dimethylarginine; CD40L, soluble CD40 ligand; CPAP, continuous positive airway pressure; NOx, nitric oxide compounds; sFasL, soluble Fas ligand; TBARS, thiobarbituric acid reactive substance. $^{*}P < 0.05$, $^{**}P < 0.01$.

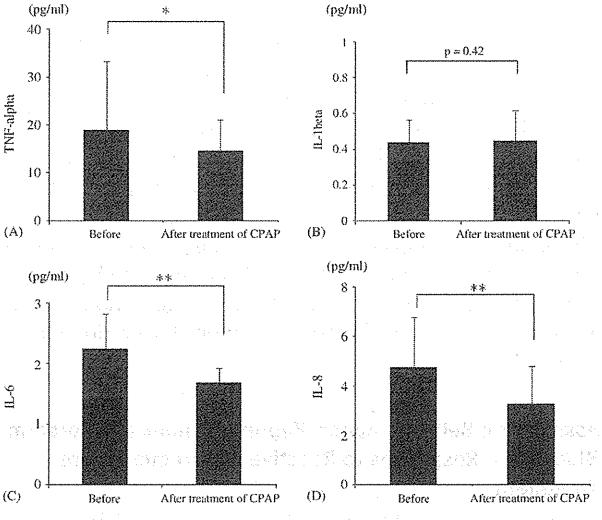

Figure 4. Alterations in the plasma levels of TNF-α (A), IL-1β (B), IL-6 (C), and IL-8 (D) in each group. Abbreviations: CPAP, continuous positive airway pressure; IL, interleukin; TNF, tumor necrosis factor. $^{*}P < 0.05$, $^{**}P < 0.01$.

in the forearm vascular function, with the patients appearing to develop potent anti-inflammatory and antiapoptotic activities.

Table 2. Multivariate Stepwise Regression Analysis of Improvement of Forearm Blood Flow Responses to Reactive Hyperemia

	Odds Ratio	*P* Value	95% CI
ΔNO	0.04	0.002	0.01–0.06
ΔADMA	−7.41	0.007	−12.63 to −2.20
ΔIL-6	−0.49	0.052	−1.00 to 0.01
ΔTNF-α	−0.07	0.006	−0.12 to −0.02

Abbreviations: ADMA, asymmetrical dimethylarginine; CI, confidence interval; IL, interleukin; NO, nitric oxide; TNF, tumor necrosis factor. Δ represents increment.

The Metabolic Syndrome, Obstructive Sleep Apnea Syndrome, and Endothelial Function

Obstructive sleep apnea syndrome and the MetS are well-established CV risk factors for the development of atherosclerosis. The prevalence of OSAS is also a risk factor for the development of hypertension and diabetes mellitus.[15] Previous studies have also shown the presence of endothelial dysfunction in patients with the MetS[16,17] or OSAS.[18] However, little is known regarding the impact of these 2 diseases on vascular function and biochemical changes and their influence on the pathogenesis of future CV risk. It has been proposed that endothelial dysfunction plays a pathogenic role in the early manifestation of atherosclerotic vascular disease and may predict future CV events. This supports the concept that abnormalities in the endothelium are one of the earliest manifestations of vasculopathies. The response of FBF to RH is considered to be a marker of endothelial function.[13,19,20]

Effect of Continuous Positive Airway Pressure on Endothelial Dysfunction, Oxidative Stress, and Biomarkers

Continuous positive airway pressure therapy prevents apneas and associated oxygen desaturation, and there is growing evidence that the treatment has long-term benefits on CV morbidity and mortality. A 7-year follow-up study carried out by Peker et al[7] showed an increased incidence of CV disease in OSAS patients whose treatment was incomplete compared with those who were treated efficiently. Furthermore, a reduction in CV deaths was observed in OSAS patients treated with CPAP compared with untreated patients over an average follow-up of 7.5 years.[8] Similarly, in a large CV outcome study with a 10-year follow-up period, severe untreated OSAS significantly increased the risk of fatal and nonfatal CV events.[9] These data suggest there is a selective and dose-dependent activation of inflammatory pathways by intermittent hypoxia/reoxygenation and support a specific role for this event in the pathophysiology of CV complications in OSAS.

In vitro investigations have shown sustained hypoxia activates hypoxia-inducible factor-1–dependent transcription, whereas intermittent hypoxia selectively activates nuclear factor κB (NFκB)-dependent transcription.[21] In OSAS patients, the levels of C-reactive protein, IL-6, and 8-hydroxydeoxyguanosine (8-OHdG) are increased compared with control subjects and are proportional to the severity of AHI.[22,23] Moreover, the relationship between expression of endothelial nitric oxide synthase (eNOS), phosphorylated eNOS, nitrotyrosine, and NFκB and the severity of OSAS has been identified, with the expression of eNOS and phosphorylated eNOS increasing, whereas expression of nitrotyrosine and NFκB and the levels of C-reactive protein and IL-6 decrease in patients with OSAS using CPAP.[23,24] Measuring the level of TBARS is a method for monitoring lipid peroxidation, a major indicator of oxidative stress. Oxidative stress increases Fas ligand expression in endothelial cells,[25] and it has been reported that the plasma level of sFasL correlates with the forearm RH in patients with coronary artery disease.[26] Hypoxia and subsequent reoxygenation induce signal transducer and activator of transcription 1 (STAT1),[27] which in turn stimulates expression of proapoptotic genes such as Fas and Fas L.[28] The effects of CPAP may therefore alter its role against stress in the progressive stages of CV disease. The findings of the present study demonstrate that CPAP treatment for 3 months effectively improves endothelial function in patients with the MetS and OSAS who have an increased risk of developing deteriorative atherosclerotic diseases. The study also suggests that improving endothelial dysfunction using CPAP therapy may reduce CV events by suppressing oxidative stress, inflammation, and apoptosis. These mechanisms may also be associated with improved FBF responses and inflammation in patients with the MetS and OSAS using CPAP.

Study Limitations

This was a preliminary, single-arm study carried out for only 3 months in a small number of subjects. A multicenter, large-scale, comparative study over a longer period is therefore needed in the future, although it is difficult to subject patients to CPAP in a randomized placebo-controlled study, as it is well established that the procedure is one of the most beneficial therapies for OSAS. However, we found significant effects of CPAP, not only on AHI, but also on changes in plasma levels of TBARS and inflammatory cytokines in patients with OSAS and the MetS.

Conclusion

We demonstrated that CPAP therapy improves endothelial dysfunction and decreases the levels of oxidative stress and inflammatory cytokines in patients with the MetS and OSAS. As endothelial function provides a prognostic marker of atherosclerotic CV disease, our data suggest that CPAP may be helpful for preventing the progressive development of atherogenic risk factors in patients with the MetS and OSAS.

Acknowledgements

The authors thank Keiko Tsuchida, Sachiyo Taguchi, and Yasuko Ueda for their expert technical assistance during the study.

References

1. Gami AS, Witt BJ, Howard DE, et al. Metabolic syndrome and risk of incident cardiovascular events and death: a systematic review and meta-analysis of longitudinal studies. *J Am Coll Cardiol.* 2007;49:403–414.

DOI:10.1002/clc.21010

2. McCurry J. Japanese people warned to curb unhealthy lifestyles: health experts urge a return to dietary basics to prevent future health problems. *Lancet.* 2004;363:1126.
3. Punjabi NM, Caffo·BS, Goodwin JL, et al. Sleep-disordered breathing and mortality: a prospective cohort study. *PLoS Med.* 2009;6:e1000132.
4. Peppard PE, Young T, Palta M, et al. Prospective study of the association between sleep-disordered breathing and hypertension. *N Engl J Med.* 2000;342:1378–1384.
5. Nieto FJ, Young TB, Lind BK, et al. Association of sleep-disordered breathing, sleep apnea, and hypertension in a large community-based study: Sleep Heart Health Study. *JAMA.* 2000;283:1829–1836.
6. Shahar E, Whitney CW, Redline S, et al. Sleep-disordered breathing and cardiovascular disease: cross-sectional results of the Sleep Heart Health Study. *Am J Respir Crit Care Med.* 2001;163:19–25.
7. Peker Y, Hedner J, Norum J, et al. Increased incidence of cardiovascular disease in middle-aged men with obstructive sleep apnea: a 7-year follow-up. *Am J Respir Crit Care Med.* 2002;166:159–165.
8. Doherty LS, Kiely JL, Swan V, et al. Long-term effects of nasal continuous positive airway pressure therapy on cardiovascular outcomes in sleep apnea syndrome. *Chest.* 2005;127:2076–2084.
9. Marin JM, Carrizo SJ, Vicente E, et al. Long-term cardiovascular outcomes in men with obstructive sleep apnoea-hypopnoea with or without treatment with continuous positive airway pressure: an observational study. *Lancet.* 2005;365:1046–1053.
10. Shamsuzzaman AS, Gersh BJ, Somers VK. Obstructive sleep apnea: implications for cardiac and vascular disease. *JAMA.* 2003;290:1906–1914.
11. Johns MW. A new method for measuring daytime sleepiness: the Epworth Sleepiness Scale. *Sleep.* 1991;14:540–545.
12. American Academy of Sleep Medicine Task Force. Sleep-related breathing disorders in adults: recommendations for syndrome definition and measurement techniques in clinical research. The Report of an American Academy of Sleep Medicine Task Force. *Sleep.* 1999;2:667–689.
13. Oyama J, Maeda T, Sasaki M, et al. Green tea catechins improve human forearm vascular function and have potent anti-inflammatory and anti-apoptotic effects in smokers. *Intern Med.* 2010;49:2553–2559.
14. Oyama J, Maeda T, Kouzuma K, et al. Green tea catechins improve human forearm endothelial dysfunction and have antiatherosclerotic effects in smokers. *Circ J.* 2010;74:578–588.
15. Parati G, Lombardi C, Narkiewicz K. Sleep apnea: epidemiology, pathophysiology, and relation to cardiovascular risk. *Am J Physiol Regul Integr Comp Physiol.* 2007;293:R1671–R1683.
16. Lind L. Endothelium-dependent vasodilation, insulin resistance and the metabolic syndrome in an elderly cohort: the Prospective Investigation of the Vasculature in Uppsala Seniors (PIVUS) study. *Atherosclerosis.* 2008;196:795–802.
17. Title LM, Lonn E, Charbonneau F, et al. Relationship between brachial artery flow mediated dilatation, hyperemic shear stress, and the metabolic syndrome. *Vasc Med.* 2008;13:263–270.
18. Chung S, Yoon IY, Shin YK, et al. Endothelial dysfunction and inflammatory reactions of elderly and middle-aged men with obstructive sleep apnea syndrome. *Sleep Breath.* 2009; 13:11–17.
19. Tagawa T, Imaizumi T, Endo T, et al. Role of nitric oxide in reactive hyperemia in human forearm vessels. *Circulation.* 1994;90:2285–2290.
20. Higashi Y, Sasaki S, Nakagawa K, et al. Effect of the angiotensin-converting enzyme inhibitor imidapril on reactive hyperemia in patients with essential hypertension: relationship between treatment periods and resistance artery endothelial function. *J Am Coll Cardiol.* 2001;37:863–870.
21. Ryan S, Taylor CT, McNicholas WT. Selective activation of inflammatory pathways by intermittent hypoxia in obstructive sleep apnea syndrome. *Circulation.* 2005;112:2660–2667.
22. Shamsuzzaman AS, Winnicki M, Lanfranchi P, et al. Elevated C-reactive protein in patients with obstructive sleep apnea. *Circulation.* 2002;105:2462–2464.
23. Yokoe T, Minoguchi K, Matsuo H, et al. Elevated levels of C-reactive protein and interleukin-6 in patients with obstructive sleep apnea syndrome are decreased by nasal continuous positive airway pressure. *Circulation.* 2003;107:1129–1134.
24. Jelic S, Lederer DJ, Adams T, et al. Vascular inflammation in obesity and sleep apnea. *Circulation.* 2010;121:1014–1021.
25. Suzuki M, Aoshiba K, Nagai A. Oxidative stress increases Fas ligand expression in endothelial cells. *J Inflamm (Lond).* 2006; 3:11.
26. Blanco-Colio LM, Martín-Ventura JL, Tuñón J, et al. Soluble Fas ligand plasma levels are associated with forearm reactive hyperemia in subjects with coronary artery disease: a novel biomarker of endothelial function? *Atherosclerosis.* 2008;201:407–412.
27. Terui K, Haga S, Enosawa S, et al. Hypoxia/re-oxygenation-induced, redox-dependent activation of STAT1 (signal transducer and activator of transcription 1) confers resistance to apoptotic cell death via hsp70 induction. *Biochem J.* 2004;380(part 1):203–209.
28. Stephanou A, Scarabelli TM, Brar BK, et al. Induction of apoptosis and Fas receptor/Fas ligand expression by ischemia/reperfusion in cardiac myocytes requires serine 727 of the STAT-1 transcription factor but not tyrosine 701. *J Biol Chem.* 2001;276: 28340–28347.

Published online in Wiley Online Library (wileyonlinelibrary.com)
DOI:10.1002/clc.21010

Repetitive hyperthermia attenuates progression of left ventricular hypertrophy and increases telomerase activity in hypertensive rats

Jun-ichi Oyama, Toyoki Maeda, Makoto Sasaki, Yoshihiro Higuchi, Koichi Node and Naoki Makino

Am J Physiol Heart Circ Physiol 302:H2092-H2101, 2012. First published 16 March 2012; doi:10.1152/ajpheart.00225.2011

Am J Physiol Heart Circ Physiol 302: H2092–H2101, 2012.
First published March 16, 2012; doi:10.1152/ajpheart.00225.2011.

Repetitive hyperthermia attenuates progression of left ventricular hypertrophy and increases telomerase activity in hypertensive rats

Jun-ichi Oyama,[1] Toyoki Maeda,[1] Makoto Sasaki,[1] Yoshihiro Higuchi,[1] Koichi Node,[2] and Naoki Makino[1]

[1]*Department of Cardiovascular, Respiratory, and Geriatric Medicine, Kyushu University Hospital at Beppu and Medical Institute of Bioregulation, Kyushu University, Oita; and* [2]*Department of Cardiovascular Medicine, Saga University, Saga, Japan*

Submitted 7 March 2011; accepted in final form 1 March 2012

Oyama J, Maeda T, Sasaki M, Higuchi Y, Node K, Makino N. Repetitive hyperthermia attenuates progression of left ventricular hypertrophy and increases telomerase activity in hypertensive rats. *Am J Physiol Heart Circ Physiol* 302: H2092–H2101, 2012. First published March 16, 2012; doi:10.1152/ajpheart.00225.2011.—We investigated the hypothesis that repetitive hyperthermia (RHT) attenuates the progression of cardiac hypertrophy and delays the transition from hypertensive cardiomyopathy to heart failure in Dahl salt-sensitive (DS) hypertensive rats. Six-week-old DS rats were divided into the following five groups: a normal-salt diet (0.4% NaCl) (NS group), a normal-salt diet plus RHT by daily immersion for 10 min in 40°C water (NS+RHT group), a high-salt diet (8% NaCl) (HS group), a high-salt diet (8% NaCl) plus RHT (HS+RHT group), and high-salt diet (8% NaCl) plus RHT with 17-DMAG (HSP90 inhibitor) administration (HS+RHT+17-DMAG group). All rats were killed at 10 wk. Cardiac hypertrophy and fibrosis were noted in the HS group, whereas RHT attenuated salt-induced cardiac hypertrophy, myocardial and perivascular fibrosis, and blood pressure elevation. The phosphorylated endothelial nitric oxide synthase (eNOS) and Akt were decreased in the HS group compared with the NS group, but these changes were not observed in the HS+RHT group. The levels of HSP60, 70, and 90 were elevated by RHT. Moreover, the increased levels of iNOS, nitrotyrosine, Toll-like receptor-4, BNP, PTX3, and TBARS in the HS group were inhibited by RHT. Telomeric DNA length, telomerase activity, and telomere reverse transcriptase (TERT) were reduced in the HS group; however, these changes were partially prevented by hyperthermia. In conclusion, RHT attenuates the development of cardiac hypertrophy and fibrosis and preserves telomerase, TERT activity and the length of telomere DNA in salt-induced hypertensive rats through activation of eNOS and induction of HSPs.

cardiac hypertrophy; endothelial nitric oxide synthase; oxidative stress; telomere; heat shock protein

HYPERTENSION IS ONE OF MAJOR risk factors responsible for cardiovascular disease and may lead to cardiac hypertrophy and diastolic heart failure (DHF). DHF is defined as heart failure with preserved left ventricular (LV) contraction and is characterized by abnormal relaxation and/or increased stiffness of the LV leading to impaired filling during diastole. Typically, diastolic function is evaluated by the E/A ratio using echocardiography. LV diastolic dysfunction is often manifested in individuals with hypertension. About 30–40% of heart failure cases occur in patients with diastolic dysfunction and normal systolic function (28, 36). Cardiac hypertrophy and resultant fibrosis develop as an adaptive response to pressure overload in hypertension and are commonly associated with DHF. Progressive cardiac remodeling characterized by LV hypertrophy, chamber enlargement, and pump dysfunction occurs in response to hypertension and is accompanied by progressive accumulation of the extracellular matrix (36).

Hyperthermia using dry sauna improves cardiac function and may also improve diastolic dysfunction in patients with congestive heart failure (CHF) (13, 44). However, little is known about possible beneficial effects of hyperthermia on hypertension-induced cardiac hypertrophy. Therefore, we investigated the effects of repetitive hyperthermia (RHT) induced by immersion in a heated water bath on LV remodeling, oxidative stress, inflammation, and telomere biology in Dahl salt-sensitive (DS) rats fed a high-salt (HS) diet, a well-established animal model of hypertensive heart disease.

METHODS

All procedures were carried out according to the protocols approved by the Institutional Committee for the Use and Care of Laboratory Animals of Kyushu University. The authors had full access to the data and take full responsibility for its integrity. All authors have read and agreed to the article as it has been written.

Animal preparation. Male DS rats (Kyudo, Fukuoka, Japan) were handled in accordance with the guidelines of Kyushu University, Graduate School of Medicine, as well as with the Guide for the Care and Use of Laboratory Animals (National Institutes of Health). The rats were individually housed in a temperature-controlled animal facility and fed a normal diet from weaning until 6 wk of age. At 6 wk of age, the rats were divided into five groups and fed a phytoestrogen-free normal-salt (NS, 0.4% NaCl) or an HS (8% NaCl) diet for the following 4 wk (Fig. 1*A*). The rats in the NS+RHT, HS+RHT, or HS+RHT+17-DMAG group were treated with RHT for 4 wk. In those groups receiving the treatment of hyperthermia, the rats were placed in the animal holder that was used for tail-cuff plethysmography and immersed in a head-up position at a 30° angle to the horizontal in a polycarbonate water bath. The lower half of the rat's body was immersed in tap water heated to 40°C for 10 min daily for 4 wk (Fig. 1*B*). All rats tolerated the immersion protocol well throughout the study. In the HS+RHT+17-DMAG group, the rats received 17-DMAG, a novel heat shock protein (HSP) 90 inhibitor (LKT Laboratories, St. Paul, MN) at the dose of 0.5 mg/kg/day by osmotic minipumps (ALZA, Palo Alto, CA) from 6 wk of age for 4 wk subcutaneously. All rats were evaluated 1 day after finishing the whole protocol.

Echocardiographic and hemodynamic measurements. Systolic blood pressure (SBP) and heart rate were measured weekly in conscious animals by tail-cuff plethysmography (Muromachi Kikai, Tokyo, Japan). Transthoracic M-mode and Doppler echocardiographic studies were carried out when the rats were 10 wk of age after they were anesthetized by intraperitoneal injection of pentobarbital sodium (50 mg/kg), using an ultrasonographic system (LogiQ 400 Pro; GE Yokogawa Medical Systems, Tokyo, Japan) with a 12-MHz trans-

Address for reprint requests and other correspondence: J.-i. Oyama, Dept. of Cardiovascular, Respiratory and Geriatric Medicine, Kyushu Univ. Hospital at Beppu & Medical Inst. of Bioregulation, Kyushu Univ., 4546 Tsurumihara, Beppu, Oita, 874-0838, Japan (e-mail: joyama@tsurumi.beppu.kyushu-u.ac.jp).